

ASSESSING SPATIO-TEMPORAL PATTERNS OF FOREST DECLINE ACROSS A  
DIVERSE LANDSCAPE IN THE KLAMATH MOUNTAINS USING A 28-YEAR  
LANDSAT TIME-SERIES ANALYSIS

By

Drew Stephen Bost

A Thesis Presented to

The Faculty of Humboldt State University

In Partial Fulfillment of the Requirements for the Degree

Master of Science in Biology

Committee Membership

Dr. Erik S. Jules, Committee Chair

Dr. Paul E. Bourdeau, Committee Member

Dr. Ramona J. Butz, Committee Member

Dr. Buddhika D. Madurapperuma, Committee Member

Dr. Erik S. Jules, Program Graduate Coordinator

December 2018

## ABSTRACT

### ASSESSING SPATIO-TEMPORAL PATTERNS OF FOREST DECLINE ACROSS A DIVERSE HETEROGENEOUS LANDSCAPE IN THE KLAMATH MOUNTAINS USING A 28-YEAR LANDSAT TIME-SERIES ANALYSIS

Drew Stephen Bost

Rates of tree mortality in California and the Pacific Northwest have greatly increased in recent years, driven largely by pest and pathogen outbreaks as well as the effects of hotter, warmer droughts. While there have been a multitude of regional-scale assessments of mortality and forest decline, landscape-level studies are necessary to better identify forests that are most vulnerable to decline and to anticipate future changes. This need is particularly notable in the remote and little-studied mountains of northwest California, which are renowned for their diverse, heterogeneous vegetation types. A recent observation of elevated levels of Shasta red fir (*Abies magnifica* var. *shastensis*) mortality in a central part of this region – the Russian Wilderness – appears to mirror the timing of these larger forest mortality events and has highlighted the need to investigate if recent levels of mortality are historically unusual. The main objectives of my study were to (1) characterize contemporary tree mortality and determine potential drivers of that mortality using field-measured data, (2) integrate both field-measured data and annual LandTrendr data to assess temporal and spatial patterns of the extent and magnitude of forest decline, (3) assess the relationship between topographic and structural attributes

with forest decline, and (4) determine whether climate is a potential driver of forest decline. To characterize contemporary tree mortality and determine potential drivers of that mortality, I established 142 field plots in the summer of 2015 measuring tree health and presence of any pests and pathogens on canopy tree species. Next, I used annualized LandTrendr algorithms across a 28-year time period (1986-2014) coupled with a regional forest type map to determine the timing, extent, and magnitude of canopy decline within each forest type. To assess potential drivers of canopy decline and identify specific vulnerabilities to drought, I used PRISM climate data and random forest classification using topographic and stand structure attributes. Plot data showed the highest proportions of mortality occurred in subalpine fir (*Abies lasiocarpa*, 35.3%) and Shasta red fir (28.6%), with evidence of fir engraver beetle (*Scolytus ventralis*) and Wien's dwarf mistletoe (*Arceuthobium abietinum* subsp. *wiensii*) on many Shasta red fir individuals (34.7% and 20.4%, respectively). Forest decline was five times higher in the last two years of the time series (2013-2014) than in the previous twenty-six years. The greatest magnitude of decline was found in the red fir and subalpine conifer forest types, findings supported by my field-measured data. Canopy decline was greater at higher elevations, in denser canopies and in stands with larger trees. I did not detect any relationships between annual climate variables and forest decline, possibly due to a discrepancy between the coarse spatial scale of the climate data and fine-grained scale of forest disturbance, or because only two years exhibited pronounced canopy decline. My study demonstrates effectiveness in characterizing forest decline in a highly diverse landscape using a remote

sensing approach and highlights the complexity of climate, pests and pathogens, stand structure, and topography as they relate to tree mortality and forest decline.

## ACKNOWLEDGEMENTS

I would like to thank my advisor Dr. Erik Jules for helping me structure and design my thesis and giving me invaluable feedback throughout the entire process. Thanks to my committee, Dr. Buddhika Madurapperuma, Dr. Paul Bourdeau, and Dr. Ramona Butz for giving me feedback and insight into various aspects of my thesis. I would also like to thank Dr. Matthew Reilly for helping me implement methodology into my thesis crucial to my final results, as well as providing feedback on numerous drafts throughout the process. I would like to thank Rocio Cristal for her loving support and patience, especially in those times I was convinced I would not finish. Thank you to my friends and family for their continued support and advice, and to the entire samba community for giving me an outlet to express myself and exist outside of my research. My thesis was funded in part through the US Forest Service (Agreement #11-CS-11051000-023) and the Agricultural Research Institute (Agreement 15-06-007).

## TABLE OF CONTENTS

ABSTRACT.....	ii
ACKNOWLEDGEMENTS.....	v
LIST OF TABLES.....	vii
LIST OF FIGURES.....	viii
INTRODUCTION.....	1
MATERIALS AND METHODS.....	7
Study Area.....	7
Field Sampling.....	8
Remote Sensing.....	9
Climate.....	11
Random Forest.....	12
RESULTS.....	15
Plot Data.....	15
LandTrendr Analysis.....	16
Climate Analyses.....	17
Random Forest Analysis.....	17
DISCUSSION.....	19
LITERATURE CITED.....	36

## LIST OF TABLES

Table 1. Summary data on forest types for the Russian Wilderness, CA. Plots were taken in the summer of 2015. Number of pixels refers to the coverage of the Landsat dataset. Elevation was calculated using a 30 m DEM. ....	26
Table 2. Pearson product-moment correlation coefficients describing the relationship between climate variables and the proportion of area experiencing decline within each forest type. Correlations were adjusted for multiple comparisons using a Bonferroni correction (n=28). All analyses were performed in R version 3.3.3.....	27

## LIST OF FIGURES

Figure 1. Map of the study area in the Russian Wilderness, CA, located within the southeastern extent of the Klamath Region (shown on locator map). Plot data was collected in summer of 2015. Vegetation type data is from the 2014 CALVEG dataset (Parker and Matyas 1979). .....	28
Figure 2. Comparison of basal area (BA) among four vegetation types in the Russian Wilderness based on 116 field-measured plots. Vegetation types were derived from combined CALVEG forest classes (see text for details). Plots were taken in summer of 2015.....	29
Figure 3. Proportion of area experiencing canopy decline for each year of the LandTrendr time series for combined forest types. Disturbance values were based on a 25-unit or greater decrease in tasseled cap wetness (TCW) between each year. Disturbance values were highest in the last two years of the time series.....	30
Figure 4. Proportion of area disturbed for each year of the LandTrendr time series for each forest type. Note the elevated levels of disturbance in the red fir and subalpine conifer forest types.....	31
Figure 5. Plot of random forest variable importance, where %IncMSE is the percentage increase in mean squared error of each explanatory variable in the random forest model. ....	32
Figure 6. Partial dependency plots for each explanatory variable included in the random forest model. Plots indicate the dependence of the model on each variable after holding all other variables at their average. The dotted line represents the TCW disturbance cutoff at a 25 unit-change. Distribution of pixel values shown as grey fill behind graphs. ....	33
Figure 7. Map of the Russian Wilderness, CA depicting canopy decline using tasseled cap wetness between 2011 and 2014. Gaps indicate non-forested areas.....	34
Figure 8. Comparison of climate variables across the time series. Size of dots indicate proportion of canopy loss for that year. ....	35

## INTRODUCTION

Recent warming temperatures and reduced precipitation in western North America have produced longer and hotter droughts, leading to marked increases in tree mortality (Allen et al. 2010). The physiological stress of drought weakens tree defenses to pests and pathogens, making them more likely to die from infestation or infection (Anderegg et al. 2012, Park Williams et al. 2013). Coupled with the shortening of bark beetle life cycles caused by rising temperatures, elevated background mortality rates and massive tree die-off events are occurring with greater frequency (van Mantgem et al. 2009, Bentz et al. 2010, Reilly and Spies 2015, Hart et al. 2017). Climate-induced mortality can cause large shifts in species composition as well as changes in ecosystem structure and function (Klos et al. 2009, van der Molen et al. 2011). In California, the unprecedented four-year drought of 2011-2015 has heightened concerns about tree mortality and has demonstrated the effects drought can have on forest ecosystems (Griffin and Anchukaitis 2014, Young et al. 2017). These effects should vary significantly depending on regional topographic characteristics, the extent of the climate event, and legacies of past land management (e.g., fire suppression), yet research exploring these interactions remains scarce (Allen et al. 2010).

Some regions experiencing widespread tree mortality events and forest decline associated with climate change have garnered significant attention among researchers, land managers and the public (e.g., Guarín and Taylor 2005, van Mantgem and Stephenson 2007, Battles et al. 2008). For example, several recent studies in the Sierra

Nevada document an increase in both stand-replacing, high severity fires and bark beetle activity over the last several decades resulting in substantial tree mortality (Smith et al. 2005, Miller et al. 2009). Drought and climate change are significant causes of these recent mortality events, raising concern for other regions of California and the Pacific Northwest (Martin et al. 2018, Bell et al. 2018). Other regions such as Colorado and Wyoming that are dominated by monospecific lodgepole pine (*Pinus contorta*) forests have seen large outbreaks of mountain pine beetle (*Dendroctonus ponderosae*) associated with decreased winter snowpack (Biederman et al. 2014). Similarly, British Columbia saw a massive mountain pine beetle outbreak between 1999 and 2015 spurred by consecutively warmer than average winters (Williams & Liebhold 2002). While studying these events has been important for our understanding of climate-driven mortality, other regions have received far less attention. Landscapes with high levels of taxonomic diversity and topographic complexity offer great opportunities for assessing how forest mortality is affected by local site characteristics, and yet these regions are the least represented in the literature.

The Klamath Mountains of northern California and southwestern Oregon are renowned for their high level of taxonomic diversity and diverse mosaic of vegetation types (Whittaker 1960, Stebbins and Major 1965, Sawyer 2007). This remote region contains ten federally-designated wilderness areas and is characterized by complex parent materials and topography, coupled with steep climatic gradients that give rise to a region with exceptionally high endemism and plant species richness (Coleman and Kruckeberg 1999). Although fire has historically been an important type of forest disturbance (Taylor

and Skinner 2003), and much of the tree mortality-related research in this region has focused on the effects of wildfires on vegetation communities (Odion et al. 2004, Miller et al. 2009), recent studies have documented more subtle changes in vegetation associated with climate change (Copeland et al. 2016, DeSiervo et al. 2018). Observations have been made in the Russian Wilderness, a small wilderness area within the Klamath Mountains (Figure 1), documenting an ongoing mortality event primarily effecting Shasta red fir (*Abies magnifica* var. *shastensis*), a variety of the red fir complex that is a hybrid between California red fir (*A. magnifica* var. *magnifica*) and noble fir (*A. procera*), a more northern species (Oline 2008). Mortality of Shasta red fir was found to be associated with fir engraver (*Scolytus ventralis*), a native bark beetle species, and Wien's dwarf mistletoe (*Arceuthobium abietinum* subsp. *wiensii*), a parasitic subspecies that primarily infests true fir hosts (DeSiervo et al. 2018). Shasta red fir mortality was also associated with an increase in minimum winter temperature between historical (1951-1980) and recent (2004-2014) time periods, highlighting the complex interactions between, pests, pathogens, and climate as they relate to tree mortality. While that study was effective in documenting the potential biotic drivers of mortality, it relied on field measurements that provided a single-year snapshot of current conditions, with no way to assess when this mortality event might have begun or how it compared to earlier levels of mortality. In general, the limitations of this and other field-based studies lie in the inability to detect the timing and spatial patterns of mortality. The use of remote sensing offers a unique perspective into the dynamics of forest disturbance and climatic drivers of

ecosystem change by assessing both the timing and spatial patterns of mortality on a broader scale than what field-measured data offers by itself.

Remote sensing has proven to be a highly effective means to quantify and assess tree mortality and forest disturbance (Kennedy et al. 2012, Meddens et al. 2013, Cohen et al. 2016). Remote sensing data is available from many sources, each with their own benefits and drawbacks depending on the image quality, spectral resolution, and desired spatiotemporal scale. Moderate Resolution Imaging Spectroradiometer (MODIS) data, for example, is limited in its spatial resolution (250-1000 m) but offers high temporal resolution with images taken twice a day, making it most useful in broad-scale analyses that require frequent coverage such as fire disturbance or pest outbreaks (Kennedy et al. 2009, Mildrexler et al. 2009, Sulla-Menashe 2014, van Lierop 2015). In contrast, many private remote sensing data sources such as DigitalGlobe's GeoEye, IKONOS, and Quickbird satellites are available at high spatial resolution but often lack the temporal and spectral resolution found in other coarser datasets (Kennedy et al. 2009). Landsat Thematic Mapper (TM) images offer an effective compromise between spatial and temporal resolution, providing data at a scale of 30 m every 16 days. This moderate spatial resolution and large temporal availability makes Landsat an ideal dataset for analyzing large-scale forest mortality and changes in forest cover over time (Kennedy et al. 2009).

Landsat time series analysis, whereby annual, pixel-based change is detected through tracking spectral trajectories across a landscape, is frequently used to detect forest disturbance and decline (Morawitz et al. 2006, Goodwin et al. 2008, Wulder et al.

2008, Vogelmann et al. 2009, Meddens et al. 2012, Van Gunst et al. 2016, Potter 2016, Cohen et al. 2016). Landsat-based detection of Trends in Disturbance and Recovery (LandTrendr) is a time series analysis tool developed to detect more subtle changes in forest health and to remove some of the year-to-year variance associated with time series analyses (Kennedy et al. 2010). LandTrendr has been used effectively to map forest decline particularly among forests in the Pacific Northwest (Kennedy et al. 2012, Cohen et al. 2010, Meigs et al. 2011 Bell et al. 2018). Bright et al. (2014) used a combination of Lidar, LandTrendr, and Aerial Detection Survey (ADS) datasets to predict live and dead basal area within five bark beetle-affected forests, showing low to moderate success in predicting tree mortality, potentially due to errors in plot sampling characteristics, ADS subjectivity, or detection of other types of disturbance in LandTrendr datasets. Kennedy et al. (2012) used LandTrendr to develop disturbance and growth maps covering the entire Northwest Forest Plan that were used to answer monitoring questions related to the distribution and timing of forest disturbance. Meigs et al. (2015) assessed mountain pine beetle and western spruce budworm (*Choristoneura freemani*) outbreaks across Oregon and Washington using a combination of LandTrendr, aerial detection survey (ADS) and plot inventory data to compare the timing and extent of each insect's disturbance. To date there has been no published research assessing long-term vegetative change using remote sensing focusing primarily on the Klamath Mountains.

The objective of this study was to quantify temporal patterns of forest decline in the Russian Wilderness using a Landsat time-series analysis. In the face of recent major droughts in California and the Pacific Northwest region, understanding how forests may

be impacted by projected changes in climate, and the associated changes in pest and pathogen loads, will be critical to help land managers make informed decisions. By coupling annualized Landsat images and climate data across 28 years (1986-2014), stratified using mapped vegetation classes, I assessed the degree of mortality among forest types using a host of different climatic and topographic variables. Specifically, the main objectives of my study were to (1) characterize contemporary tree mortality and determine potential drivers of that mortality using field-measured data, (2) integrate both field-measured data and annual LandTrendr data to assess temporal and spatial patterns of the extent and magnitude of forest decline, (3) assess the relationship between topographic and structural attributes with forest decline, and (4) determine whether climate is a potential driver of forest decline. Based on my previous field observations, I predicted that forests dominated by Shasta red fir would show the largest signals of recent mortality. In addition, I expected to detect that drought and increasing temperatures were drivers of this mortality.

## MATERIALS AND METHODS

### Study Area

The study site was located in the Russian Wilderness, a 51 km<sup>2</sup> wilderness area in northern California within the Klamath National Forest (41°17'N, 122°57'W) (Figure 1). The Russian Wilderness was designated by the United States Forest Service (USFS) in 1984, consisting of moderate to high elevations in mountainous terrain ranging from 760-2,500 m and comprised of granodiorite parent material. This wilderness provides a unique study area for documenting changes in forest structure due in part to its high diversity of conifer species and vegetation types (Sawyer and Thornburgh 1974). There are 18 documented conifer species within the wilderness boundaries, representing one of the highest densities of conifer taxa on record (Kauffmann 2012). Common forest types range from lower elevation mixed conifer forest containing ponderosa pine (*Pinus ponderosa*), lodgepole pine (*Pinus contorta*), and Douglas-fir (*Pseudotsuga menziesii*); upper elevation mixed conifer forests containing white fir (*Abies concolor*), Shasta red fir (*Abies magnifica* var. *shastensis*), western white pine (*Pinus monticola*) and mountain hemlock (*Tsuga mertensiana*); and subalpine forest types dominated by whitebark pine (*Pinus albicaulis*) (Sawyer and Thornburgh 1971, Sawyer and Thornburgh 1974). This botanical diversity was the primary reason that portions of the wilderness were also designated as Forest Service Management Areas, split between the southern Sugar Creek

Research Natural Area (RNA) and the northern Duck Lake Botanical Area (Sawyer and Thornburgh 1971, Keeler-Wolf 1984).

### Field Sampling

To characterize contemporary tree mortality and determine potential drivers, field plots were established in the summer of 2015 as part of a previous study documenting recent tree mortality in the Russian Wilderness (DeSiervo et al. 2018). Plot locations were originally determined based on a resampling project of a 1969 dataset to document the unique vegetation types within the wilderness area (Sawyer and Thornburgh 1974). The 2015 dataset consisted of 142 fixed-radius plots with radii of 11.37 m (0.04 ha). Plots were geolocated and differentially corrected using a Trimble GPS (Juno 3B, Trimble Navigation, Ltd., Sunnyvale, California, USA). Within each plot, information was recorded on species, status (live, unhealthy, and dead), and presence of all identifiable forest insects and pathogens for each canopy tree, defined as any tree  $\geq 7.6$  cm diameter at breast height (dbh) and  $\geq 1.37$  m tall. The designation of “unhealthy” was assigned to trees with substantial physical damage (either mechanically or biotically generated) and poor or very poor crown vigor. Only plots that were within the four main forest types were included (see below), for a total of 116 plots (Table 1). Species with less than 60 individuals were removed from the dataset to ensure more accurate comparison between species. Tree measurements were summarized by live, unhealthy, and dead basal area (BA) in units of  $\text{m}^2$  for each species and within each plot.

## Remote Sensing

Because my study focused primarily on conifer tree mortality and disturbance, the study area was divided into dominant forest cover types using the Classification and Assessment with Landsat of Visible Ecological Groupings (CALVEG) system. CALVEG uses Landsat spectral signatures to determine vegetation types across the state of California (Parker and Matyas 1979). To simplify comparison among forest types, the original CALVEG classifications were reduced from nine to four dominant overstory groupings: subalpine conifer, red fir, mixed conifer, and white fir. The groupings were made by manually assessing CALVEG's original vegetation descriptions and combining forest types that had similar understory and overstory species composition and elevation ranges. For example, the subalpine conifer forest type is a combination of the subalpine conifer and mountain hemlock cover types. Combined categories were also compared to field-measured species composition and cover class to ensure that new categories were accurately represented (Figure 2).

Landsat TM, ETM+ and OLI 8 images were selected within the growing season (June-August) between the years of 1986 and 2014. I chose 2014 as the cutoff year because of a wildfire that burned through a portion of the study area in late 2014. Images were processed using the LandTrendr algorithms which are described in detail in Kennedy et al. (2010). Briefly, multiple georectified Landsat images were selected and aggregated for each year of the time series. Radiometric normalization was done using the multivariate alteration detection and calibration (MADCAL) algorithm described by

Canty et al. (2004) to remove the effects of atmospheric scattering. Radiometrically corrected Landsat images were then used to calculate the three tasseled-cap (TC) bands of brightness (TCB), greenness (TCG) and wetness (TCW) using the formula defined by Crist and Cicone (1984). Only TCW was used for the analysis given its sensitivity to detecting vegetation vigor (Skakun et al. 2003, Meddens et al. 2013). Once the Landsat image stack was normalized and TC indices calculated, the LandTrendr temporal segmentation algorithm was fitted to each image. This fitting process smooths the usually noisy year-to-year trajectory of pixels throughout the time series to allow for more accurate classification of disturbed and undisturbed pixels. Finally, the entire image stack was clipped using the four CALVEG forest types.

To assess the relative change of TCW values throughout the time series,  $\Delta$ TCW images were calculated by differencing each sequential LandTrendr image in the image stack. Any pixel showing a decrease in TCW value was classified as experiencing canopy decline. To reduce commission errors due to left-over atmospheric scattering or background noise, a cutoff value was set at a 25-unit decrease. Meigs et al. (2011) used a cutoff value of 50 units using the Normalized Burn Ratio (NBR) for similar purposes when studying western spruce budworm and mountain pine beetle. Given the high diversity of conifer taxa in the Russian Wilderness, I expected decline values to be generally lower than that of other studies, hence my use of a lower canopy decline cutoff. To better characterize the magnitude of decline, I classified all pixels that experienced decline into the highest 25% of values and lowest 75%. Finally, the proportion of the

study area experiencing canopy decline was calculated for each of the 28 years by dividing the number of declined pixels in that year by the total number of pixels.

### Climate

Climate data was gathered from the Parameter-elevation Regression on Independent Slopes Model (PRISM, Daly et al. 2002) on a 2 km grid. PRISM interpolates climate data from a combination of instrumental records and topographic characteristics such as slope, aspect, elevation, and rain shadows. Since four PRISM cells overlapped the study area, the average was taken of the two cells that contained the majority of the study area. Climate variables were generated for each year in the time series and included: maximum growing season temperature (Jun-Aug), minimum winter temperature (Dec-Feb), total water year precipitation (Oct-Sept), and minimum and maximum growing season vapor pressure deficit. Vapor pressure deficit is used as a measure of drought severity (Seager et al. 2015, Restaino et al. 2016) and represents the difference between the amount of moisture in the air and how much moisture can be held in the air once saturated. Most climate variables were obtained for the growing season (Jun-Aug) because it represents the highest vegetation vigor of any given year and coincides with the Landsat image acquisition dates. Minimum winter temperature was chosen as it is known to affect the reproduction of certain bark beetle species (Bentz et al. 2010). Increased winter temperatures can shorten the overwintering phase of the bark beetles' life cycle and push their emergence date forward, increasing the potential for population outbreak (Christiansen et al. 1987, Bentz et al. 2010). Pearson product-

moment correlation coefficients were generated to assess the relationship of each climate variable with the proportion of the study area experiencing decline for the combined images and separately for each forest type, adjusted for multiple comparisons using a Bonferroni correction. All analyses were performed in R version 3.3.3 (R Core Development Team 2017).

### Random Forest

Random forest modeling was used to assess the effect of topographic and stand structure variables on forest decline using the Random Forest package (Liaw and Wiener 2002) for R (R Development Core Team 2017). Random forest is a non-parametric statistical method for classification and regression. The algorithm has been shown to be an effective tool for predicting ecological attributes from remotely sensed and explanatory variables (Prasad et al. 2006, Cutler et al. 2007, Dillon et al. 2011). Random forest iteratively and randomly samples the dataset to produce a large number of classifications, represented by decision trees, from which a final classification is chosen, representing the mode of all created decision trees. This final classification is weighed based on its prediction strength and error rate, with the lowest error rates selected as the strongest classifiers. Some benefits of using random forest over other statistical methods include its' ability to find relationships among continuous, non-normal variables and ranking of explanatory variables based on their classification importance.

The response variable used in the model was a differenced TCW image between the years of 2011 and 2014, a period that represents the greatest decrease in TCW values

across the time series. Topographic explanatory variables used in the random forest model included elevation, slope, transformed aspect (Beers et al. 1966), Heat Load Index (HLI, Jenness 2006) and Topographic Position Index (TPI, Jenness 2006). HLI is a measure of solar radiation in a given area and is based on aspect, slope, and coordinate position, with zero representing the coolest slopes and two representing the hottest slopes. TPI is a measure of slope position on a landscape, with lower values indicating valleys or ravines and higher values indicating ridges and hilltops. A 500 m neighborhood was ultimately determined to be the most accurate given the relatively small study area. Structural attributes included in the model were tree canopy cover class, stand structure, and vegetation type taken from the CALVEG dataset. Canopy cover is divided into three classes: sparse (10-30%), moderate (30-60%), and dense canopy cover (60-100%). Stand structure consists of five size classes: saplings (1-4.9 in. Quadratic Mean Diameter [QMD, 2.5-12.5 cm]), poles (5-9.9 in. QMD [12.7-25.1 cm]), small (10-19.9 in. QMD [25.4-50.6 cm]), medium (20-29.9 in. QMD [50.8-76 cm]), and large (30+ in. QMD [76.2 cm]). Correlations between explanatory variables were tested using Pearson correlation tests. A random sample of 5000 pixels was selected from the dataset, representing ~12% of the data. Smaller sample sizes produced highly variable random forest results when run consecutively. Default settings were applied from the random forest package: the number of variables tried at each split equaled the number of predictor variables divided by three, 500 trees were grown, and the minimum size of terminal nodes was five. Runs with a higher number of trees yielded similar results.

To assess the relative influence of individual explanatory variables on forest disturbance, variable importance rankings were calculated for each variable. Random forest calculates variable importance by randomly permuting the values of each explanatory variable and calculating the change in overall model performance, expressed as a change in average squared prediction error. Scores are assigned to each variable, ranked in order of largest to smallest percent increase in the model's mean squared error (MSE). To produce stable ranking of explanatory variables, random forest was run ten consecutive times and the average score for each variable was used to assign importance. Partial dependency plots were generated for each variable to further evaluate the interaction between disturbance, topography, and structural attributes. These plots separately show the relationship between the individual explanatory variables and canopy decline while holding all other variables in the model at their average (Cutler et al. 2007). They effectively show the model's "dependence" on each variable as it relates to the overall predictive accuracy of the model.

## RESULTS

### Plot Data

A total of 3,446 canopy trees were measured across 116 plots (Figure 1). The most abundant species sampled was white fir, followed by Shasta red fir and mountain hemlock. Across all taxa, the proportion of dead individuals was 17%. Mortality varied by species, with the highest proportions of mortality occurring in subalpine fir (*Abies lasiocarpa*, 35.3%), Shasta red fir (28.6%), and lodgepole pine (22%). The total proportion of all species designated as unhealthy was 7.2%, with the highest proportions occurring in subalpine fir (19.1%) and Shasta red fir (16.2%). Engelmann spruce (*Picea engelmannii*), Brewer spruce (*Picea breweriana*), and Douglas-fir (*Pseudotsuga menziesii*) had the lowest proportions of mortality (7.8%, 9.5%, and 10.7% respectively), and lodgepole pine, ponderosa pine, and white fir had the lowest proportions of unhealthy trees (0.8%, 1.6%, and 2.2%).

Bark beetle activity was found on 13.1% of all sampled trees, with high variation amongst species. Presence of bark beetle activity was highest among Shasta red fir (34.7%) and whitebark pine (21.3%), with nearly all galleries present on Shasta red fir identified as fir engraver beetle. For Shasta red fir, bark beetle activity was highest in the largest diameter trees (over 20 cm dbh). Fir engraver beetle galleries were identified on several dead subalpine fir and white fir individuals. Most of the bark beetle activity on whitebark pine occurred on old dead snags and were therefore difficult to identify to

species, however *Ips* spp. galleries were identified on a few individuals. Mountain pine beetle galleries were detected on some lodgepole pine snags as well as western pine beetle (*Dendroctonus brevicomis*) galleries on a few live ponderosa pine. Dwarf mistletoe was found on 14.4% of sampled trees with high variation amongst host species. Mistletoe is a hemiparasitic plant that can damage host trees when infestation is severe. Mistletoe was most abundant for ponderosa pine (24.6%), though 87% of infected trees came from a single plot. Mountain hemlock and Shasta red fir had high levels of infestation (21.7% and 20.4%, respectively), widely distributed across plots. Dwarf mistletoe was detected on all sizes classes of Shasta red fir; however infestation was most common among smaller diameter trees (<20 cm dbh).

#### LandTrendr Analysis

The proportion of the study area that experienced canopy decline varied considerably across the time series (Figure 3). The greatest proportions occurred in 2013 with 14.2% of the area experiencing decline, followed by 2014 with 14.1%. Of that area, 32% showed high levels of canopy decline in 2013, followed by and 28% in 2014, representing the greatest 25% of decline within each year. In contrast, all other years had between 1% and 5% of the area showing decline, with an average decline of 3%. A moderate pulse of canopy decline occurred between the years of 2000-2003, ranging from 4.1-4.6%. All forest types generally matched what I observed for the overall study area, with the highest levels of mortality being found in the last two years of the time series (Figure 4). The highest proportion of decline occurred in the red fir forest type,

with 16.6% of the area experiencing decline in 2013 and 17.3% in 2014. Subalpine conifer had the second highest proportions at 15.2% and 13.6% across same years. Both mixed conifer and white fir forest types had lower levels of decline in the last two years of the time series relative to other forest types (8.4-6.6% and 9.5-10.7% respectively). On average, 3.5% of the study area experienced decline across the entire time period. Of that, 25% was classified as high levels of decline.

### Climate Analyses

I observed no significant correlations between all climate variables and the estimated proportion of forest decline (Table 2). Maximum summer temperature had the strongest positive correlation coefficients across all climate variables and were highest with the subalpine conifer and mixed conifer forest types. Although minimum and maximum vapor pressure deficit had relatively stronger positive correlation coefficients among the same forest types, none were significant. Surprisingly, precipitation had the weakest correlation coefficients with little to no change across forest types. Minimum winter temperature also had weak correlations with forest decline, results that are contrary to a previous climate analysis done in this region showing positive correlations with tree mortality (DeSiervo et al. 2018).

### Random Forest Analysis

Random forest modeling explained 18.8% of the variance in canopy decline between 2011 and 2014. Importance values were consistent across all ten model

iterations and ranked elevation, slope and TPI as the three most important variables in the models (Figure 5). Elevation had a 51.6% increased MSE, followed by slope at 43.4% and TPI at 33.6% MSE. Vegetation type, aspect and HLI ranked consistently low in variable importance, adding a percent increase MSE of 25.0% and 27.1%, respectively. Canopy cover and stand structure contributed between 30-33% increases in MSE. Partial dependency plots showed the specific influence of individual topographic variables on canopy decline to vary considerably (Figure 6). Greater canopy decline occurred at higher elevations, with a sharp increase around 1,950 m and leveling off around 2,200 m. For slope, greater canopy decline occurred between 40-50°. Canopy decline varied across topographic sites (TPI), with relatively stable values up until around 150, where decline sharply increases. An increase in canopy decline occurred at southwestern aspects, with a gradual decrease towards more northeastern slopes. Surprisingly, HLI showed greater canopy decline at both warmer and cooler sites. Canopy cover and stand structure varied considerably in their effects on canopy decline. Large and medium-sized stands showed the largest increases in canopy decline, with all other categories falling below the 25-unit disturbance cutoff. Greater increases in canopy decline were also observed in denser forests (60–100% canopy cover) relative to the other cover classes.

## DISCUSSION

This study provides evidence for recent and pronounced increases in forest decline in one of the North America's most diverse forested ecosystems. By employing annualized LandTrendr algorithms to my study area across a 28-year time period, I found that levels of forest decline were five times greater in the last two years of the time series (2013-2014) than in the previous twenty-six years. Forest decline was not uniformly distributed across the Russian Wilderness landscape but differed among topographic settings and stand structural conditions. The highest levels of canopy decline were found at higher elevations in dense red fir and subalpine conifer forests with old-growth forest attributes (i.e., large-diameter trees), suggesting that these forests may be particularly vulnerable to future disturbances. My study supports the growing body of literature showing increase in tree mortality and forest decline across California and the Pacific Northwest (van Mantgem et al. 2009, Cohen et al. 2010). Many remote sensing studies occur at very broad spatial scales, covering entire ecoregions and multiple states (Meddens et al. 2013, Meigs et al. 2015, Cohen et al. 2016). My study, by contrast, focused on a much smaller and more diverse landscape, enabling greater focus on more nuanced differences in the effects of forest decline on stand structure, topography and forest type.

The increased levels of forest decline I observed using remote sensing data are supported by field-measured observations, particularly in red fir forests. Shasta red fir exhibited one of the highest amounts of both dead and unhealthy trees from the sampled

plot data (Figure 2). When assessed separately, forest types varied in the mortality they experienced. Shasta red fir had consistently high levels of mortality, even when found in other forest types and particularly within the subalpine and mixed conifer forest types (Figure 2). These results indicate that much of the disturbance being detected by LandTrendr is occurring in Shasta red fir forest types, both within Shasta red fir-dominated forests and in mixed forest types. The partial dependency plots also support this conclusion, showing forest decline dramatically increasing around 1,950 m. This is consistent with the typical elevation range of the red fir forest type, which in the Russian Wilderness averages around 1,960 m.

These findings agree with recent studies that focus specifically on red fir mortality, and provide strong evidence of increasing red fir mortality in California. Mortenson et al. (2015) examined rates of red fir mortality based on re-measured trees in Forest Inventory and Analysis (FIA) plots across all of California between the years of 2000-2010 and found an annual mortality rate of 1.8%, generally coinciding with the disturbance rates I measured over that same time period (Figure 3). Dwarf mistletoe was the most significant contributor to mortality which also supports the plot-based measurements I made, as well as previous analyses examining causal mortality agents (DeSiervo et al. 2018). That recent rates of decline are nearly five times greater than both my own measurements of mortality and those of Mortenson et al. (2015) is serious cause for concern for the health of Shasta red fir in this region. While my study focused primarily on mortality in major forest types, the plot data showed an unexpectedly high proportion of subalpine fir mortality (35%) which raises particular concern for this

species at the most southern extent of its range. Including the Russian Wilderness, subalpine fir is found in only eight separate locations in California (Kauffmann 2012). Although exact causes of mortality are difficult to discern with my small sample size, evidence of fir engraver beetle as well as balsam woolly adelgid (*Adelges piceae*) were commonly found on dead and unhealthy individuals, highlighting the vulnerability of subalpine fir to pests in this area and a threat to regional forest biodiversity.

Implementation of monitoring in other portions of the species' southern distribution may be warranted to determine the health of subalpine fir populations outside the Russian Wilderness.

Compared with the results of other remote sensing studies that used similar indices, the magnitude of disturbance I found in the Russian Wilderness is relatively low. My measured values of decline using the TCW index showed annual decreases ranging from 25-200, compared to fire disturbance studies using the NBR index which typically see differences in the 600-800 range for high severity fire (Miller et al. 2009). Fires naturally cause greater disturbance both in the amount of area effected and its severity and is therefore much more sensitive to remote sensing indices. Other remote sensing studies observing the effects of bark beetle outbreaks often involve larger outbreaks in more homogenous forest types, making detection via satellite imagery easier (Aukema et al. 2006, Verbesset et al. 2009, Dennison et al. 2010). By contrast, in highly mixed conifer forests like those found in the Russian Wilderness that are being affected by fir engraver beetle, tree mortality occurs in a more fine-grained, patchy mosaic of decline. The distribution of  $\Delta$  TCW values between 2011 and 2014 exemplifies this fine-

grained decline pattern (Figure 7), with most of the disturbance occurring in small patches alongside several larger clusters.

I found no significant relationships between the levels of forest decline and my modelled climate variables. These findings are contrary to the climate analysis done by DeSiervo et al. (2018) which found greater Shasta red fir mortality in plots with higher minimum temperatures. The differences may be associated with the scale of these analyses; DeSiervo et al. (2018) used plot-specific measurements of climate, whereas I used averaged climate data for the entire study area. This smaller scale may resolve differences in climatic conditions that I was unable to detect at a coarser, landscape-level scale. Small-scale climate variability may play an important role in how climate change affects certain species, however the identification of climate refugia is difficult and has largely been descriptive (Morelli et al. 2016). Further research may be warranted in identifying small-scale changes in climate across heterogeneous landscapes like the Russian Wilderness.

Precipitation also showed little relationship with forest decline, a result that was consistent with the DeSiervo et al. (2018) analysis. These findings are contrary to much of the literature regarding forest mortality in California and the Pacific Northwest that predict increased levels of mortality driven by drought (van Mantgem and Stephenson 2007, Allen et al. 2015). While much of California has experienced record-setting droughts between 2011 and 2015, Rapacciuolo et al. (2014) demonstrated that precipitation patterns across the region are geographically variable, with some areas of the Klamath showing increases in precipitation while others show little to no change. The

simplicity of my climate analysis may also be contributing to a lack of significant relationships between forest decline and climate. Because the study area has only two years with large disturbance values (2013-2014), a correlation test may not be able to adequately assess significant relationships (see Figure 8). These results further exemplify the complexity of the interactions between climate and forest disturbance and warrant further research.

Fire suppression may be partially responsible for some of the recent conifer mortality occurring in my study area. Land managers have been actively suppressing wildfires in conifer forests of California and the Pacific Northwest for over a century, leading to massive fuel accumulation and increases in stand density (McKelvey et al. 1996, Gruell 2001, DiMario et al. 2018). Prior to active fire exclusion, forests in the Klamath Mountains region were characterized by a mixed-severity fire regime, with a high frequency of low to moderate severity fires in mixed conifer forests (Skinner et al. 2006, Safford et al. 2011). Prior to late summer of 2014, this region of the Klamath had not experienced a wildfire in over 100 years, with low- and mid- elevation vegetation types missing the most fire cycles (Safford and Van de Water 2014). Increased stand density from fire suppression has been shown to cause mortality through higher competition among trees (Guarín and Taylor 2005, Maloney 2011, Millar et al. 2012), findings that are supported by my random forest results that show higher disturbance values among denser forests (Figure 6). These denser stands can also increase the spread of pests and pathogens. Furthermore, the interaction of increased pest and pathogen

spread coupled with increased stand competition may be some of the leading causes of the mortality observed in the Russian Wilderness.

When analyzing stand structure attributes, the greatest decreases in canopy decline I observed occurred in the large and medium size classes, as well as in the largest canopy cover class (60-100%, Figure 6). These observations indicate that mortality is occurring in dense, old-growth stands where pests and pathogens have an easier time spreading between hosts. Field measurements also supported this observation, where the proportion of Shasta red fir with signs of bark beetles was greater in larger size classes (>20 cm dbh, DeSiervo et al. 2018). These findings are consistent with recent research highlighting the vulnerability of old-growth stands to climate change and pests (Battles et al. 2008, Allen et al. 2015). A study conducted by van Mantgem et al. (2009) documented a steady increase in background mortality rates of old-growth forests driven primarily by regional warming and water deficits from the mid-1950s to late 2000s. The elevated rates of decline I observed are consistent with those found by van Mantgem et al. (2009), particularly the moderate increase in mortality rates from 2000-2005 ranging from a 3-6% increase. While these background rates of mortality are consistent between the two studies, van Mantgem et al.'s (2009) study did not assess the extreme drought California experienced in 2011 and my observed levels of forest decline increased in 2013 and 2014. It should also be noted that van Mantgem et al. (2009) had different methods of data collections and overall objectives than my study, making direct comparison of results difficult. Regardless, this dramatic increase in forest decline we document raises concern for the health of conifer forests in the Russian Wilderness.

This study provides valuable insight into a recent mortality event in a highly diverse conifer forest of northern California. The use of remote sensing data provided a broader context for what might have been demonstrated using only field-collected data. Remote sensing analyses allow researchers to gain a broader understanding, both temporally and spatially, of forest decline trends. My study highlights trends of forest decline in high elevations species, specifically Shasta red fir and subalpine fir, and highlights the need for more research and monitoring to be conducted regarding the casual agents driving this mortality. A more comprehensive study of the interactions between climate and forest disturbance may expose some potential correlations not found in my analysis. Long-term monitoring may also allow a better link between field-derived measurements and remote sensing data and would allow stronger confidence as to the drivers of tree mortality in the Russian Wilderness. This work contributes to the growing body of evidence indicating increased levels of mortality among forests of western North America, and the roles climate, pest and pathogens, and topography play in driving and shaping this mortality across a diverse and heterogeneous landscape.

Table 1. Summary data on forest types for the Russian Wilderness, CA. Plots were taken in the summer of 2015. Number of pixels refers to the coverage of the Landsat dataset. Elevation was calculated using a 30 m DEM.

Forest Type	# Plots	# Pixels	Elevation (m)	Total area (m <sup>2</sup> )
Mixed Conifer	12	4,604	1539-2326	138,120
White Fir	23	7,068	1480-2243	212,040
Red Fir	45	20,048	1561-2313	601,440
Subalpine Conifer	36	10,642	1703-2482	319,260

Table 2. Pearson product-moment correlation coefficients describing the relationship between climate variables and the proportion of area experiencing decline within each forest type. Correlations were adjusted for multiple comparisons using a Bonferroni correction (n=28). All analyses were performed in R version 3.3.3.

Climate Variable	White fir	Mixed conifer	Subalpine conifer	Red fir	Combined
Minimum winter temperature	-0.03	0.12	0.16	0.09	0.10
Maximum summer temperature	0.27	0.36	0.40	0.33	0.35
Minimum vapor pressure deficit	0.20	0.43	0.37	0.31	0.19
Maximum vapor pressure deficit	0.10	0.27	0.24	0.18	0.33
Total water year precipitation	-0.11	0.07	0.00	0.00	-0.01

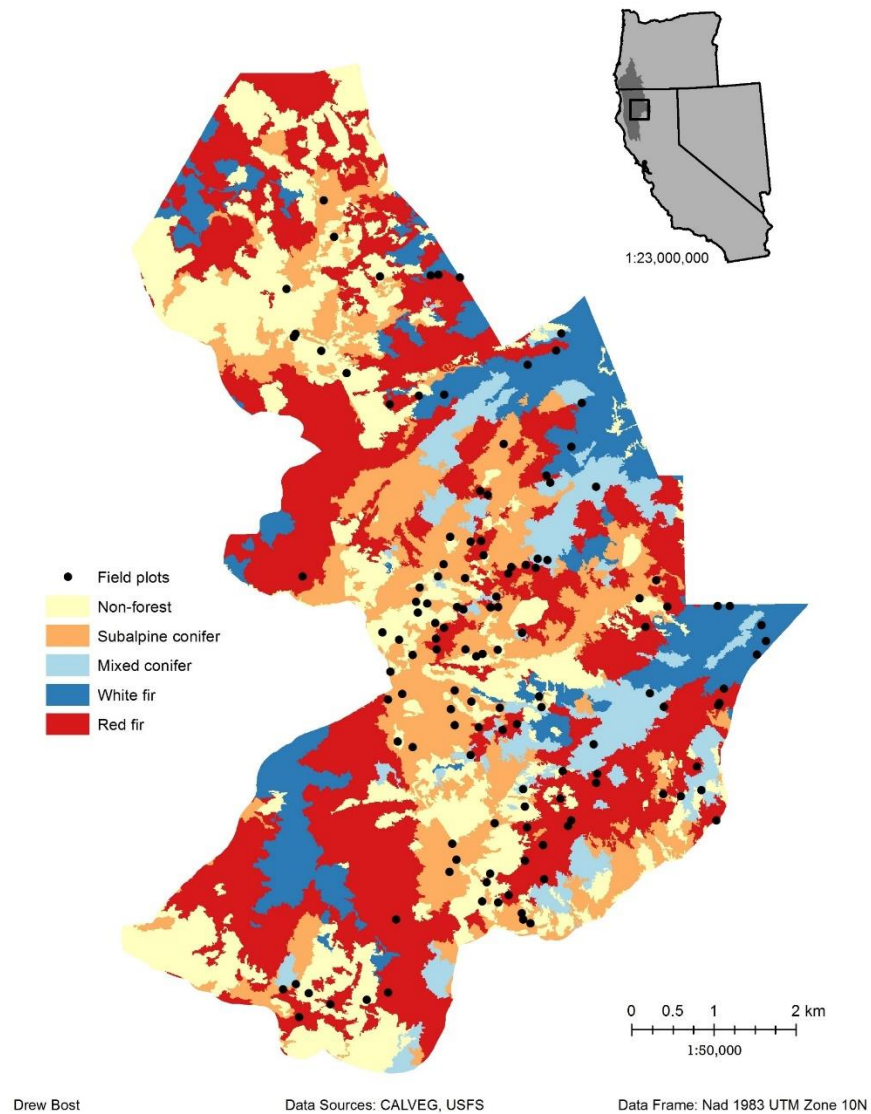


Figure 1. Map of the study area in the Russian Wilderness, CA, located within the southeastern extent of the Klamath Region (shown on locator map). Plot data was collected in summer of 2015. Vegetation type data is from the 2014 CALVEG dataset (Parker and Matyas 1979).

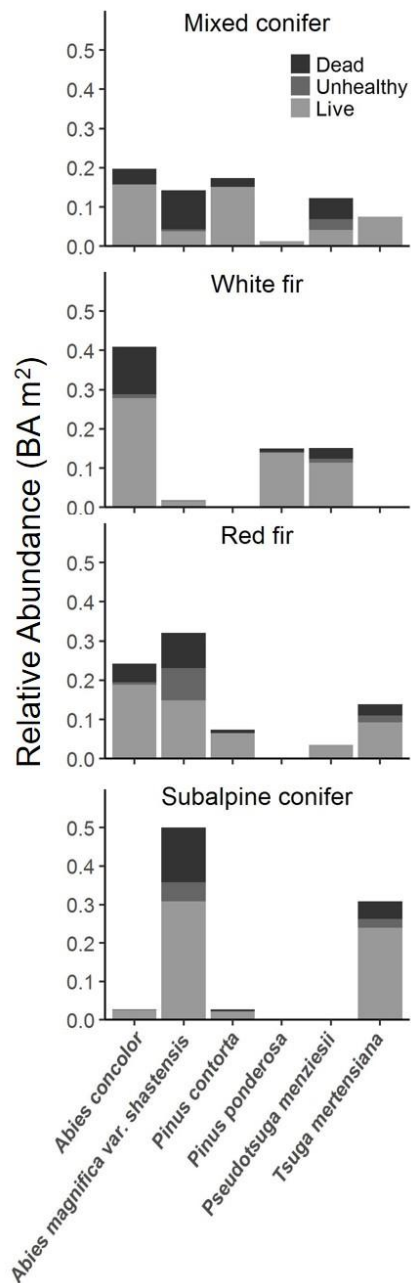


Figure 2. Comparison of basal area (BA) among four vegetation types in the Russian Wilderness based on 116 field-measured plots. Vegetation types were derived from combined CALVEG forest classes (see text for details). Plots were taken in summer of 2015.

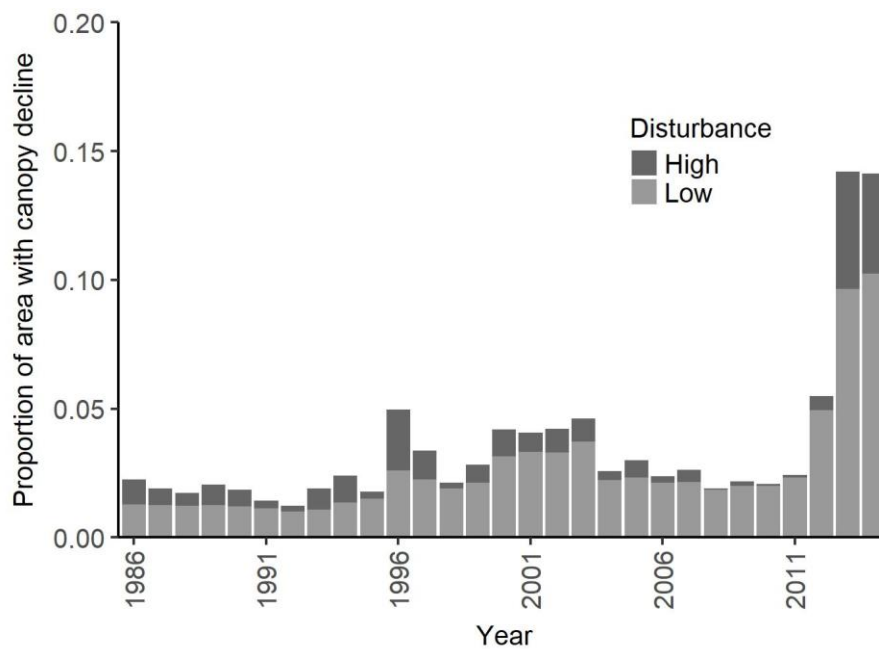


Figure 3. Proportion of area experiencing canopy decline for each year of the LandTrendr time series for combined forest types. Disturbance values were based on a 25-unit or greater decrease in tasseled cap wetness (TCW) between each year. Disturbance values were highest in the last two years of the time series.

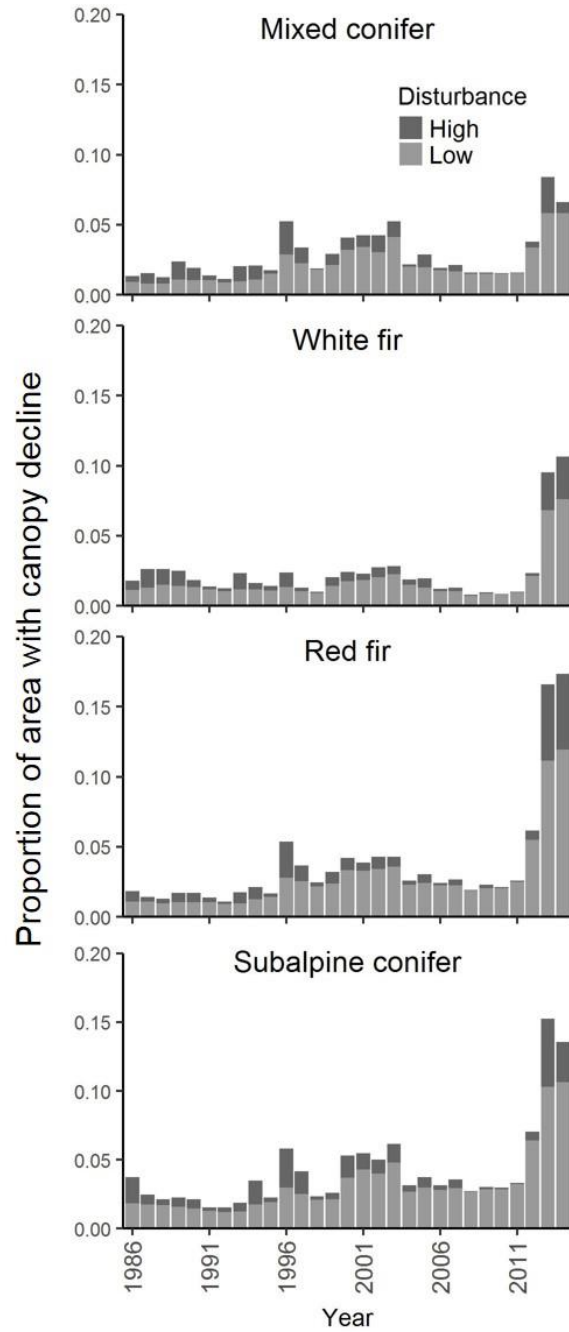


Figure 4. Proportion of area disturbed for each year of the LandTrendr time series for each forest type. Note the elevated levels of disturbance in the red fir and subalpine conifer forest types.

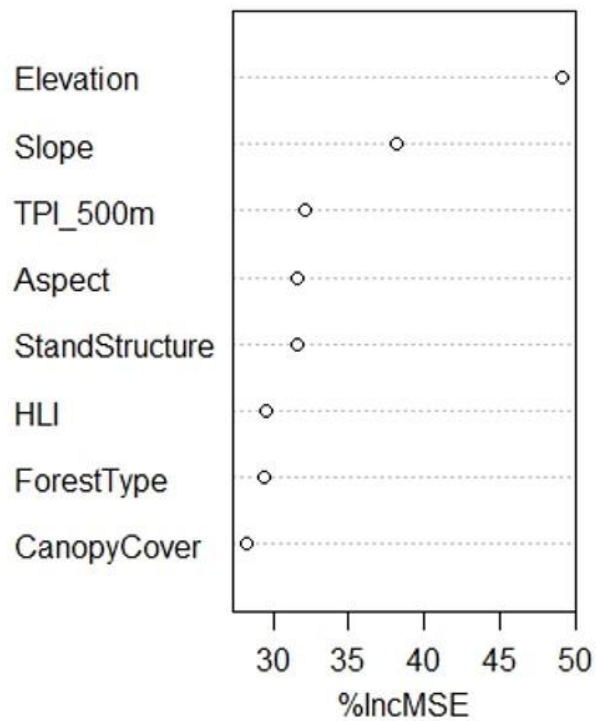


Figure 5. Plot of random forest variable importance, where %IncMSE is the percentage increase in mean squared error of each explanatory variable in the random forest model.

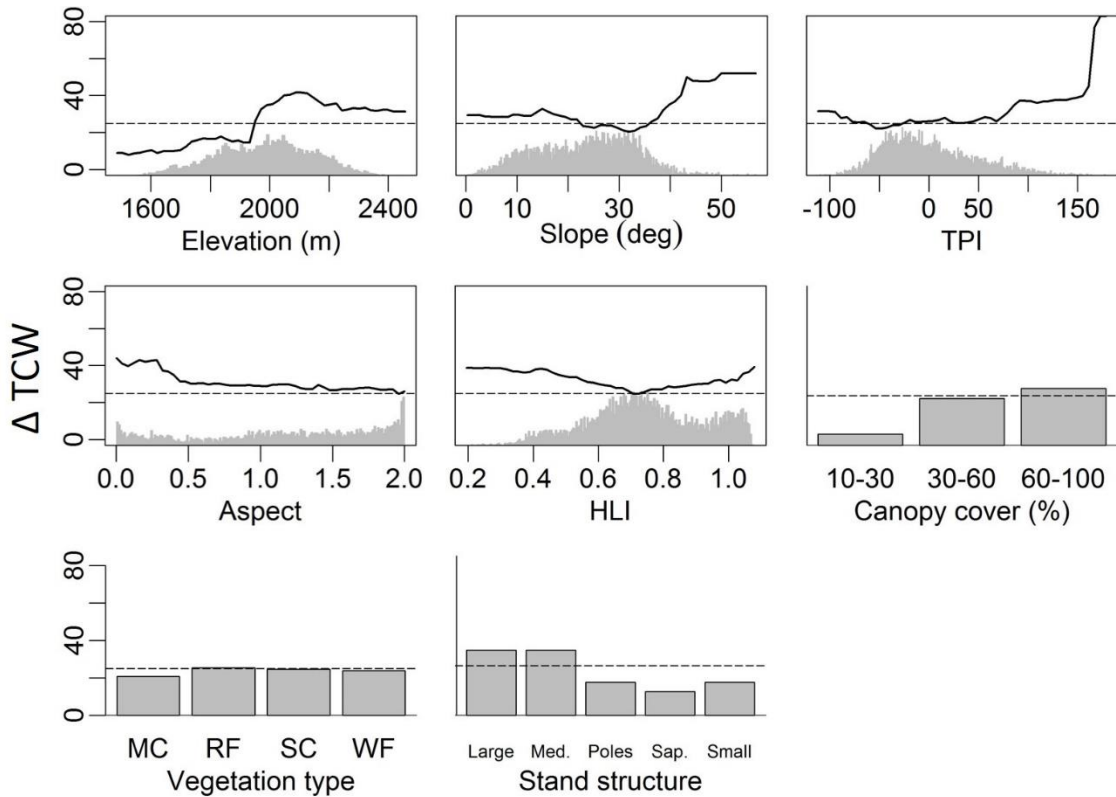


Figure 6. Partial dependency plots for each explanatory variable included in the random forest model. Plots indicate the dependence of the model on each variable after holding all other variables at their average. The dotted line represents the TCW disturbance cutoff at a 25 unit-change. Distribution of pixel values shown as grey fill behind graphs.

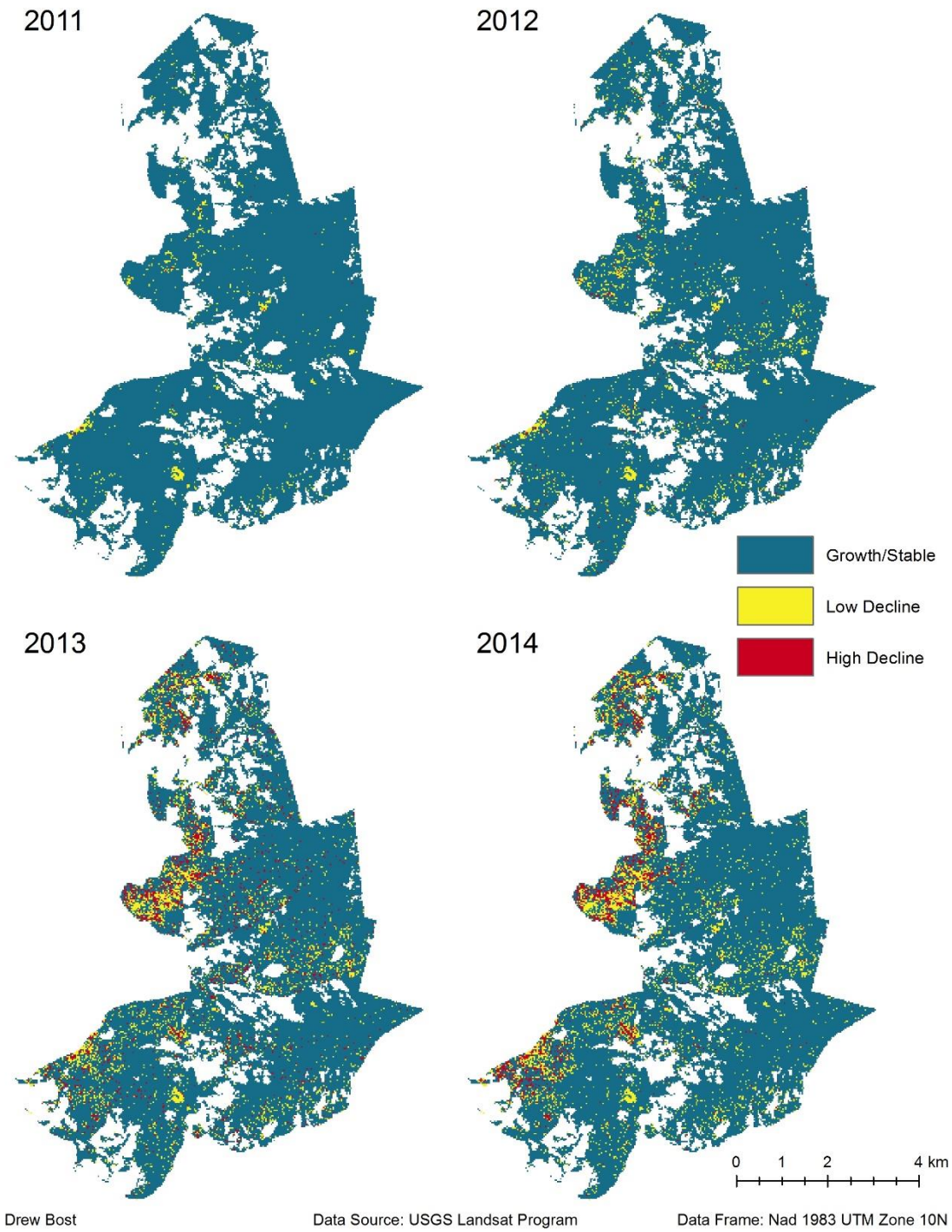


Figure 7. Map of the Russian Wilderness, CA depicting canopy decline using tasseled cap wetness between 2011 and 2014. Gaps indicate non-forested areas.

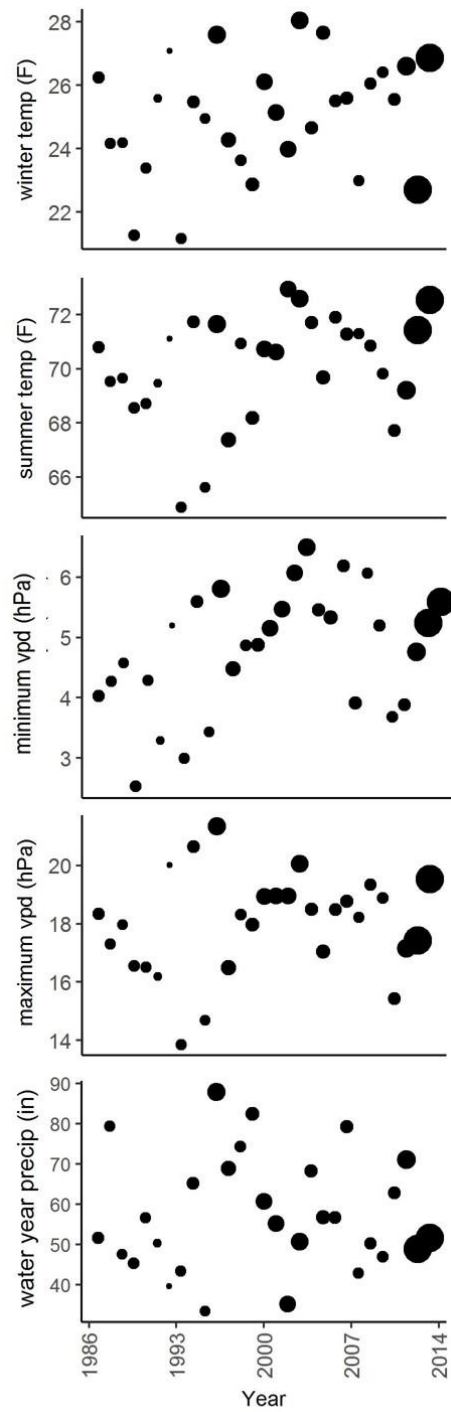


Figure 8. Comparison of climate variables across the time series. Size of dots indicate proportion of canopy loss for that year.

## LITERATURE CITED

- Allen, C. D., Breshears, D. D., & McDowell, N. G. (2015). On underestimation of global vulnerability to tree mortality and forest die-off from hotter drought in the Anthropocene. *Ecosphere*, 6(8), 1–55.
- Allen, C. D., Macalady, A. K., Chenchouni, H., Bachelet, D., McDowell, N., Vennetier, M., ... Cobb, N. (2010). A global overview of drought and heat-induced tree mortality reveals emerging climate change risks for forests. *Forest Ecology and Management*, 259(4), 660–684. <https://doi.org/10.1016/j.foreco.2009.09.001>
- Anderegg, W. R. L., Kane, J. M., & Anderegg, L. D. L. (2012). Consequences of widespread tree mortality triggered by drought and temperature stress. *Nature Climate Change*, 3(1), 30–36. <https://doi.org/10.1038/nclimate1635>
- Aukema, B. H., Carroll, A. L., Zhu, J., Raffa, K. F., Sickley, T. A., & Taylor, S. W. (2006). Landscape level analysis of mountain pine beetle in British Columbia, Canada: spatiotemporal development and spatial synchrony within the present outbreak. *Ecography*, 29(3), 427–441.
- Battles, J. J., Robards, T., Das, A., Waring, K., Gilless, J. K., Biging, G., & Schurr, F. (2008). Climate change impacts on forest growth and tree mortality: a data-driven modeling study in the mixed-conifer forest of the Sierra Nevada, California. *Climatic Change*, 87(S1), 193–213. <https://doi.org/10.1007/s10584-007-9358-9>
- Beers, T.W., Dress, P.E. & Wensel, L.C. 1966. Aspect trans-formation in site productivity research. *J. For.* 64: 691.
- Bell, D. M., Cohen, W. B., Reilly, M., & Yang, Z. (2018). Visual interpretation and time series modeling of Landsat imagery highlight drought's role in forest canopy declines. *Ecosphere*, 9(6), e02195. <https://doi.org/10.1002/ecs2.2195>
- Bentz, B. J., Régnière, J., Fettig, C. J., Hansen, E. M., Hayes, J. L., Hicke, J. A., ... Seybold, S. J. (2010). Climate Change and Bark Beetles of the Western United States and Canada: Direct and Indirect Effects. *BioScience*, 60(8), 602–613. <https://doi.org/10.1525/bio.2010.60.8.6>
- Biederman, J. A., Brooks, P. D., Harpold, A. A., Gochis, D. J., Gutmann, E., Reed, D. E., ... Ewers, B. E. (2014). Multiscale observations of snow accumulation and peak snowpack following widespread, insect-induced lodgepole pine mortality. *Ecohydrology*, 7(1), 150–162. <https://doi.org/10.1002/eco.1342>

- Bright, B. C., Hudak, A. T., Kennedy, R. E., & Meddens, A. J. H. (2014). Landsat Time Series and Lidar as Predictors of Live and Dead Basal Area Across Five Bark Beetle-Affected Forests. *IEEE Journal of Selected Topics in Applied Earth Observations and Remote Sensing*, 7(8), 3440–3452. <https://doi.org/10.1109/JSTARS.2014.2346955>
- Canty, M. J., Nielsen, A. A., & Schmidt, M. (2004). Automatic radiometric normalization of multitemporal satellite imagery. *Remote Sensing of Environment*, 91(3), 441–451. <https://doi.org/10.1016/j.rse.2003.10.024>
- Christiansen, E., Waring, R. H., & Berryman, A. A. (1987). Resistance of conifers to bark beetle attack: Searching for general relationships. *Forest Ecology and Management*, 22(1–2), 89–106. [https://doi.org/10.1016/0378-1127\(87\)90098-3](https://doi.org/10.1016/0378-1127(87)90098-3)
- Cohen, W. B., Yang, Z., & Kennedy, R. (2010). Detecting trends in forest disturbance and recovery using yearly Landsat time series: 2. TimeSync — Tools for calibration and validation. *Remote Sensing of Environment*, 114(12), 2911–2924. <https://doi.org/10.1016/j.rse.2010.07.010>
- Cohen, W. B., Yang, Z., Stehman, S. V., Schroeder, T. A., Bell, D. M., Masek, J. G., ... Meigs, G. W. (2016). Forest disturbance across the conterminous United States from 1985–2012: The emerging dominance of forest decline. *Forest Ecology and Management*, 360, 242–252. <https://doi.org/10.1016/j.foreco.2015.10.042>
- Coleman, R. G., & Kruckeberg, A. R. (1999). Geology and plant life of the Klamath-Siskiyou Mountain region. *Natural Areas Journal*, 19(4), 320–340.
- Copeland, S. M., Harrison, S. P., Latimer, A. M., Damschen, E. I., Eskelinen, A. M., Fernandez-Going, B., ... Thorne, J. H. (2016). Ecological effects of extreme drought on Californian herbaceous plant communities. *Ecological Monographs*, 86(3), 295–311. <https://doi.org/10.1002/ecm.1218>
- Crist, E. P., & Cicone, R. C. (1984). A Physically-Based Transformation of Thematic Mapper Data—The TM Tasseled Cap. *IEEE Transactions on Geoscience and Remote Sensing*, GE-22(3), 256–263. <https://doi.org/10.1109/TGRS.1984.350619>
- Cutler, D. R., Edwards, T. C., Beard, K. H., Cutler, A., Hess, K. T., Gibson, J., & Lawler, J. J. (2007). Random Forests for Classification in Ecology. *Ecology*, 88(11), 2783–2792. <https://doi.org/10.1890/07-0539.1>
- Daly, C., Gibson, W. P., Taylor, G. H., Johnson, G. L., & Pasteris, P. (2002). A knowledge-based approach to the statistical mapping of climate. *Climate Research*, 22(2), 99–113. <https://doi.org/10.3354/cr022099>

- Dennison, P. E., Brunelle, A. R., & Carter, V. A. (2010). Assessing canopy mortality during a mountain pine beetle outbreak using GeoEye-1 high spatial resolution satellite data. *Remote Sensing of Environment*, 114(11), 2431–2435.  
<https://doi.org/10.1016/j.rse.2010.05.018>
- DeSiervo, M. H., Jules, E. S., Bost, D. S., Stigter, D., L, E., & Butz, R. J. (2018). Patterns and Drivers of Recent Tree Mortality in Diverse Conifer Forests of the Klamath Mountains, California. *Forest Science*. <https://doi.org/10.1093/forsci/fxx022>
- Dillon, G. K., Holden, Z. A., Morgan, P., Crimmins, M. A., Heyerdahl, E. K., & Luce, C. H. (2011). Both topography and climate affected forest and woodland burn severity in two regions of the western US, 1984 to 2006. *Ecosphere*, 2(12), 1–33.  
<https://doi.org/10.1890/ES11-00271.1>
- DiMario, A. A., Kane, J. M., & Jules, E. S. (2018). Characterizing Forest Floor Fuels Surrounding Large Sugar Pine (*Pinus lambertiana*) in the Klamath Mountains, California. *Northwest Science*, 92(3), 181-190.
- Existing Vegetation - CALVEG, [ESRI personal geodatabase]. (2004). McClellan, CA: USDA-Forest Service, Pacific Southwest Region. EvegTile03B\_99\_04\_v2. [2009].
- Goodwin, N. R., Coops, N. C., Wulder, M. A., Gillanders, S., Schroeder, T. A., & Nelson, T. (2008). Estimation of insect infestation dynamics using a temporal sequence of Landsat data. *Remote Sensing of Environment*, 112(9), 3680–3689.  
<https://doi.org/10.1016/j.rse.2008.05.005>
- Griffin, D., & Anchukaitis, K. J. (2014). How unusual is the 2012-2014 California drought?: GRIFFIN AND ANCHUKAITIS. *Geophysical Research Letters*, 41(24), 9017–9023.  
<https://doi.org/10.1002/2014GL062433>
- Gruell, G. E. (2001). *Fire in Sierra Nevada forests: a photographic interpretation of ecological change since 1849*. Mountain Press.
- Guarín, A., & Taylor, A. H. (2005). Drought triggered tree mortality in mixed conifer forests in Yosemite National Park, California, USA. *Forest Ecology and Management*, 218(1–3), 229–244. <https://doi.org/10.1016/j.foreco.2005.07.014>
- Hart, S. J., Veblen, T. T., Schneider, D., & Molotch, N. P. (2017). Summer and winter drought drive the initiation and spread of spruce beetle outbreak. *Ecology*, 98(10), 2698–2707.  
<https://doi.org/10.1002/ecy.1963>
- Jenness, J. (2006). Topographic Position Index (tpi\_jen.avx) extension for ArcView 3.x, v. 1.3a. Jenness Enterprises.

- Kauffmann, M. E. (2012). *Conifer Country: A natural history and hiking guide to 35 conifers of the Klamath Mountain region*.
- Keeler-Wolf, T. (1984). Vegetation map of the upper Sugar Creek drainage, Siskiyou County, California. Unpublished report on file, Pacific Southwest Research Station, Albany, Calif.
- Kennedy, R. E., Townsend, P. A., Gross, J. E., Cohen, W. B., Bolstad, P., Wang, Y. Q., & Adams, P. (2009). Remote sensing change detection tools for natural resource managers: Understanding concepts and tradeoffs in the design of landscape monitoring projects. *Remote Sensing of Environment*, *113*(7), 1382–1396. <https://doi.org/10.1016/j.rse.2008.07.018>
- Kennedy, R. E., Yang, Z., & Cohen, W. B. (2010). Detecting trends in forest disturbance and recovery using yearly Landsat time series: 1. LandTrendr — Temporal segmentation algorithms. *Remote Sensing of Environment*, *114*(12), 2897–2910. <https://doi.org/10.1016/j.rse.2010.07.008>
- Kennedy, R. E., Yang, Z., Cohen, W. B., Pfaff, E., Braaten, J., & Nelson, P. (2012). Spatial and temporal patterns of forest disturbance and regrowth within the area of the Northwest Forest Plan. *Remote Sensing of Environment*, *122*, 117–133. <https://doi.org/10.1016/j.rse.2011.09.024>
- Klos, R. J., Wang, G. G., Bauerle, W. L., & Rieck, J. R. (2009). Drought impact on forest growth and mortality in the southeast USA: an analysis using Forest Health and Monitoring data. *Ecological Applications: A Publication of the Ecological Society of America*, *19*(3), 699–708.
- Liaw, A., & Wiener, M. (2002). Classification and Regression by RandomForest. *R News*, (2), 18–22.
- Maloney, P. E., Vogler, D. R., Eckert, A. J., Jensen, C. E., & Neale, D. B. (2011). Population biology of sugar pine (*Pinus lambertiana* Dougl.) with reference to historical disturbances in the Lake Tahoe Basin: implications for restoration. *Forest Ecology and Management*, *262*(5), 770-779.
- Martin, R. E., Asner, G. P., Francis, E., Ambrose, A., Baxter, W., Das, A. J., ... Stephenson, N. L. (2018). Remote measurement of canopy water content in giant sequoias (*Sequoiadendron giganteum*) during drought. *Forest Ecology and Management*, *419–420*, 279–290. <https://doi.org/10.1016/j.foreco.2017.12.002>
- McKelvey, K. S., Skinner, C. N., Chang, C., Erman, D. C., Husari, S. J., Parsons, D. J., ... Weatherspoon, C. P. (1996). An overview of fire in the Sierra Nevada. *Pages 1033-1040 in: Sierra Nevada Ecosystem Project, Final Report to Congress, Vol. II, Assessments and*

*Scientific Basis for Management Options*. Davis, CA: University of California, Centers for Water and Wildland Resources. Report No. 37. Retrieved from <https://www.fs.usda.gov/treearch/pubs/3539>

- Meddens, A. J. H., Hicke, J. A., & Ferguson, C. A. (2012). Spatiotemporal patterns of observed bark beetle-caused tree mortality in British Columbia and the western United States. *Ecological Applications*, 22(7), 1876–1891. <https://doi.org/10.1890/11-1785.1>
- Meddens, A. J. H., Hicke, J. A., Vierling, L. A., & Hudak, A. T. (2013). Evaluating methods to detect bark beetle-caused tree mortality using single-date and multi-date Landsat imagery. *Remote Sensing of Environment*, 132, 49–58. <https://doi.org/10.1016/j.rse.2013.01.002>
- Meigs, G. W., Kennedy, R. E., & Cohen, W. B. (2011). A Landsat time series approach to characterize bark beetle and defoliator impacts on tree mortality and surface fuels in conifer forests. *Remote Sensing of Environment*, 115(12), 3707–3718. <https://doi.org/10.1016/j.rse.2011.09.009>
- Meigs, G. W., Kennedy, R. E., Gray, A. N., & Gregory, M. J. (2015). Spatiotemporal dynamics of recent mountain pine beetle and western spruce budworm outbreaks across the Pacific Northwest Region, USA. *Forest Ecology and Management*, 339, 71–86. <https://doi.org/10.1016/j.foreco.2014.11.030>
- Mildrexler, D. J., Zhao, M., & Running, S. W. (2009). Testing a MODIS Global Disturbance Index across North America. *Remote Sensing of Environment*, 113(10), 2103–2117. <https://doi.org/10.1016/j.rse.2009.05.016>
- Millar, C. I., Westfall, R. D., Delany, D. L., Bokach, M. J., Flint, A. L., & Flint, L. E. (2012). Forest mortality in high-elevation whitebark pine (*Pinus albicaulis*) forests of eastern California, USA; influence of environmental context, bark beetles, climatic water deficit, and warming. *Canadian Journal of Forest Research*, 42(4), 749–765. <https://doi.org/10.1139/x2012-031>
- Miller, J. D., Safford, H. D., Crimmins, M., & Thode, A. E. (2009). Quantitative Evidence for Increasing Forest Fire Severity in the Sierra Nevada and Southern Cascade Mountains, California and Nevada, USA. *Ecosystems*, 12(1), 16–32. <https://doi.org/10.1007/s10021-008-9201-9>
- Morawitz, D. F., Blewett, T. M., Cohen, A., & Alberti, M. (2006). Using NDVI to Assess Vegetative Land Cover Change in Central Puget Sound. *Environmental Monitoring and Assessment*, 114(1–3), 85–106. <https://doi.org/10.1007/s10661-006-1679-z>

- Morelli, T. L., Daly, C., Dobrowski, S. Z., Dulen, D. M., Ebersole, J. L., Jackson, S. T., ... & Nydick, K. R. (2016). Managing climate change refugia for climate adaptation. *PLoS One*, 11(8), e0159909.
- Mortenson, L., Gray, A. N., & Shaw, D. C. (2015). A forest health inventory assessment of red fir (*Abies magnifica*) in upper montane California. *Ecoscience*, 22(1): 47-58., 22(1), 47–58. <https://doi.org/10.1080/11956860.2015.1047142>
- Odion, D. C., Frost, E. J., Strittholt, J. R., Jiang, H., Dellasala, D. A., & Moritz, M. A. (2004). Patterns of Fire Severity and Forest Conditions in the Western Klamath Mountains, California. *Conservation Biology*, 18(4), 927–936. <https://doi.org/10.1111/j.1523-1739.2004.00493.x>
- Oline, D. K. (2008). Geographic variation in chloroplast haplotypes in the California red fir-noble fir species complex and the status of Shasta red fir. *Canadian Journal of Forest Research*, 38(10), 2705–2710. <https://doi.org/10.1139/X08-097>
- Park Williams, A., Allen, C. D., Macalady, A. K., Griffin, D., Woodhouse, C. A., Meko, D. M., ... McDowell, N. G. (2013). Temperature as a potent driver of regional forest drought stress and tree mortality. *Nature Climate Change*, 3(3), 292–297. <https://doi.org/10.1038/nclimate1693>
- Parker, I., and Matyas, W. (1979). CALVEG: a classification of Californian vegetation. U.S. Department of Agriculture, Forest Service, Pacific Southwest Region Station, Albany, California.
- Potter, C. (2016). Thirty years of vegetation change in the coastal Santa Cruz Mountains of Northern California detected using landsat satellite image analysis. *Journal of Coastal Conservation*, 20(1), 51–59. <https://doi.org/10.1007/s11852-015-0417-5>
- Prasad, A. M., Iverson, L. R., & Liaw, A. (2006). Newer Classification and Regression Tree Techniques: Bagging and Random Forests for Ecological Prediction. *Ecosystems*, 9(2), 181–199. <https://doi.org/10.1007/s10021-005-0054-1>
- R Core Development Team (2017). R: A language and environment for statistical computing. R Foundation for Statistical Computing, Vienna, Austria.
- Rapacciuolo, G., Maher, S. P., Schneider, A. C., Hammond, T. T., Jabis, M. D., Walsh, R. E., ... Beissinger, S. R. (2014). Beyond a warming fingerprint: individualistic biogeographic responses to heterogeneous climate change in California. *Global Change Biology*, 20(9), 2841–2855. <https://doi.org/10.1111/gcb.12638>

- Reilly, M. J., & Spies, T. A. (2015). Regional variation in stand structure and development in forests of Oregon, Washington, and inland Northern California. *Ecosphere*, 6(10), art192. <https://doi.org/10.1890/ES14-00469.1>
- Restaino, C. M., Peterson, D. L., & Littell, J. (2016). Increased water deficit decreases Douglas fir growth throughout western US forests. *Proceedings of the National Academy of Sciences*, 113(34), 9557–9562. <https://doi.org/10.1073/pnas.1602384113>
- Safford, H. D., van de Water, K., & Schmidt, D. (2011). California Fire Return Interval Departure (FRID) map metadata: Description of purpose, data sources database fields, and their calculations. USDA Forest Service, Pacific Southwest Region, Vallejo.
- Safford, H. D., & Van de Water, K. M. (2014). Using fire return interval departure (FRID) analysis to map spatial and temporal changes in fire frequency on national forest lands in California. Res. Pap. PSW-RP-266. Albany, CA: US Department of Agriculture, Forest Service, Pacific Southwest Research Station. 59 p, 266.
- Sawyer, J. O. (2007). Why are the Klamath Mountains and adjacent North Coast floristically diverse? *Fremontia*, 35(3), 3–11.
- Sawyer, J. O.; Thornburgh, D. A. 1971. Vegetation types on granodiorite in the Klamath Mountains, California. Report to the Pacific Southwest Forest and Range Experiment Station, Berkeley, California. PSW COOP-AID agreement supplement #10. Unpublished report on file, Pacific Southwest Research Station, Albany, Calif.
- Sawyer, J. O., & Thornburgh, D. A. (1974). Subalpine And Montane Forests On Granodiorite In The Central Klamath Mountains Of California.
- Seager, R., Hooks, A., Williams, A. P., Cook, B., Nakamura, J., & Henderson, N. (2015). Climatology, Variability, and Trends in the U.S. Vapor Pressure Deficit, an Important Fire-Related Meteorological Quantity. *Journal of Applied Meteorology and Climatology*, 54(6), 1121–1141. <https://doi.org/10.1175/JAMC-D-14-0321.1>
- Skakun, R. S., Wulder, M. A., & Franklin, S. E. (2003). Sensitivity of the thematic mapper enhanced wetness difference index to detect mountain pine beetle red-attack damage. *Remote Sensing of Environment*, 86(4), 433–443. [https://doi.org/10.1016/S0034-4257\(03\)00112-3](https://doi.org/10.1016/S0034-4257(03)00112-3)
- Skinner, C. N., A. H. Taylor, and J. K. Agee. 2006. Klamath Mountain bioregion. Pages 170–194 in N. G. Sugihara, J. W. van Wagendonk, K. E. Shaffer, J. Fites-Kaufman, and A. E. Thode, editors. Fire in California's ecosystems. The University of California Press, Berkeley, California, USA.

- Smith, T. F., Rizzo, D. M., & North, M. (2005). Patterns of Mortality in an Old-Growth Mixed-Conifer Forest of the Southern Sierra Nevada, California. *Forest Science*, 51(3), 266–275.
- Stebbins, G. L., & Major, J. (1965). Endemism and Speciation in the California Flora. *Ecological Monographs*, 35(1), 1–35. <https://doi.org/10.2307/1942216>
- Sulla-Menashe, D., Kennedy, R. E., Yang, Z., Braaten, J., Krankina, O. N., & Friedl, M. A. (2014). Detecting forest disturbance in the Pacific Northwest from MODIS time series using temporal segmentation. *Remote Sensing of Environment*, 151, 114–123. <https://doi.org/10.1016/j.rse.2013.07.042>
- Taylor, A. H., & Skinner, C. N. (2003). Spatial patterns and controls on historical fire regimes and forest structure in the Klamath Mountains. *Ecological Applications*, 13(3), 704–719.
- van der Molen, M. K., Dolman, A. J., Ciais, P., Eglin, T., Gobron, N., Law, B. E., ... Wang, G. (2011). Drought and ecosystem carbon cycling. *Agricultural and Forest Meteorology*, 151(7), 765–773. <https://doi.org/10.1016/j.agrformet.2011.01.018>
- Van Gunst, K. J., Weisberg, P. J., Yang, J., & Fan, Y. (2016). Do denser forests have greater risk of tree mortality: A remote sensing analysis of density-dependent forest mortality. *Forest Ecology and Management*, 359, 19–32. <https://doi.org/10.1016/j.foreco.2015.09.032>
- van Lierop, P., Lindquist, E., Sathyapala, S., & Franceschini, G. (2015). Global forest area disturbance from fire, insect pests, diseases and severe weather events. *Forest Ecology and Management*, 352, 78–88. <https://doi.org/10.1016/j.foreco.2015.06.010>
- van Mantgem, P. J., Stephenson, N. L., Byrne, J. C., Daniels, L. D., Franklin, J. F., Fule, P. Z., ... Veblen, T. T. (2009). Widespread Increase of Tree Mortality Rates in the Western United States. *Science*, 323(5913), 521–524. <https://doi.org/10.1126/science.1165000>
- van Mantgem, Phillip J., & Stephenson, N. L. (2007). Apparent climatically induced increase of tree mortality rates in a temperate forest. *Ecology Letters*, 10(10), 909–916. <https://doi.org/10.1111/j.1461-0248.2007.01080.x>
- Verbesselt, J., Robinson, A., Stone, C., & Culvenor, D. (2009). Forecasting tree mortality using change metrics derived from MODIS satellite data. *Forest Ecology and Management*, 258(7), 1166–1173.
- Vogelmann, J. E., Tolck, B., & Zhu, Z. (2009). Monitoring forest changes in the southwestern United States using multitemporal Landsat data. *Remote Sensing of Environment*, 113(8), 1739–1748. <https://doi.org/10.1016/j.rse.2009.04.014>

- Whittaker, R. H. (1960). Vegetation of the Siskiyou Mountains, Oregon and California. *Ecological Monographs*, 30(3), 279–338. <https://doi.org/10.2307/1943563>
- Williams, David W., and Liebhold, Andrew M. (2002). Climate change and the outbreak ranges of two North American bark beetles. *Agricultural and Forest Entomology*, 4(2), 87-99.
- Wulder, M. A., White, J. C., Coops, N. C., & Butson, C. R. (2008). Multi-temporal analysis of high spatial resolution imagery for disturbance monitoring. *Remote Sensing of Environment*, 112(6), 2729–2740. <https://doi.org/10.1016/j.rse.2008.01.010>
- Young, D. J. N., Stevens, J. T., Earles, J. M., Moore, J., Ellis, A., Jirka, A. L., & Latimer, A. M. (2017). Long-term climate and competition explain forest mortality patterns under extreme drought. *Ecology Letters*, 20(1), 78–86. <https://doi.org/10.1111>